A Systematic Radiochemical Study of Photopion Nuclear Reactions of Complex Nuclei at Intermediate Energies

Koh Sakamoto[1], Hiromitsu Haba[2], Samir Ranjan Sarkar[1], Yasuji Oura[3], Hiroshi Matsumura[1], Yutaka Miyamoto[1], Seiichi Shibata[4], Michiaki Furukawa[5], and Ichiro Fujiwara[6]

[1]Department of Chemistry, Faculty of Science, Kanazawa University,
Kanazawa-shi, Ishikawa 920-1192, Japan
e-mail: kohsakamoto@par.odn.ne.jp
[2]Research Group for Nuclear Chemistry of Heavy Elements,
Advanced Science Research Center, Japan Atomic Energy Research Institute,
Tokai, Naka-gun, Ibaraki 319-1195, Japan
[3]Department of Chemistry, Graduate School of Science, Tokyo Metropolitan University,
Hachioji-shi, Tokyo 192-0397, Japan
[4]Research Reactor Institute, Kyoto University, Sennan-gun, Osaka 590-0494, Japan
[5]Faculty of Environmental and Information Sciences, Yokkaichi University,
Yokkaichi-shi, Mie 512-8512, Japan
[6]Department of Economics, Faculty of Economics, Otemon-Gakuin University,
Ibaraki-shi, Osaka 567-8502, Japan

A short review is given on our systematic studies of photopion nuclear reactions, in which the product yields from (γ,π^+) and (γ,π^-xn) reactions for x = 0–9 have been measured radiochemically as functions of bremsstrahlung end-point energy (E_0) from 30 to 1200 MeV and of target mass, ^{27}Al–^{181}Ta for (γ,π^+) and ^{7}Li–^{209}Bi for (γ,π^-xn) reactions. Yield variations as a function of the number of the emitted neutrons (x) for each target at $E_0 \geq 400$ MeV were found to be typical of (3,3) resonance. The reactions for neutron multiplicities as large as $x \geq 6$ are notable for targets of mass $A_t \geq 100$, while only the reactions for smaller x are measurable for the lighter targets. The yields for both (γ,π^-) and (γ,π^+) are A_t-independent for targets heavier than A_t > 30–40, while much smaller yields are reported for targets with A_t = 7–14. The yield ratio $(\gamma,\pi^-)/(\gamma,\pi^+)$ becomes as high as 5.5 and such a high value suggests that the neutron density in the surface region of nucleus is higher than that expected from the neutron-to-proton ratio for the entire nucleus. The observed yields for individual (γ,π^-xn) reactions having equal x were also found to be a smoothly varying function of the neutron-to-proton ratio of the target, $(N/Z)_t$, not of the target mass A_t or number of target neutrons N_t. This implies that the reactions are initiated via competitive photoabsorptions by neutrons and protons in the target nucleus. The smooth variation of the profile changes its characteristics at $(N/Z)_t$ = 1.30~1.40, corresponding to A_t = 100–130; this implies higher excitation energies due to progressively larger medium effects in nuclei with A_t > 100. The results are compared with theoretical calculations made using the photon-induced intranuclear cascade and evaporation analysis program by Gabriel and Alsmiller.

1. Introduction

At energies above the pion production thresholds, the Δ isobar is expected to be produced through (3,3) resonance absorption of an incoming photon by a single nucleon (N) in the target nucleus. The isobar decays immediately (10^{-24} s) into a stable nucleon and a pion: $\gamma + n \rightarrow \Delta^0 \rightarrow p + \pi^-$, $\gamma + p \rightarrow \Delta^+ \rightarrow n + \pi^+$, and $\gamma + N \rightarrow \Delta^0 \rightarrow N + \pi^0$. After these initial processes, pion and/or nucleon may escape from the nucleus or develop a cascade-evaporation process inside the nucleus. The probability of the escape may depend on the location of the formation of Δ, thence on the size of the nucleus. Especially, when photoabsorption occurs at the surface region of the nucleus, the chance of an escape would be high. A systematic measurement of photopion reaction yields as functions of photon energy and target mass has, therefore, been of our current interest [1–4].

Radiochemical methods are useful for identifying individual (γ,π^-xn) reactions for different x. It is possible to isolate the product nuclides chemically as a series of radioisotopes with mass numbers $(A_t–x)$ belonging to (Z_t+1) element from a target with mass number A_t of an element with atomic number Z_t and also from the dominant spallation products of $A_p < A_t$ and $Z_p \leq Z_t$. The (γ,π^+) reaction leads to a product nucleus of $A_p = A_t$ and $Z_p = Z_t–1$ that is also distinguishable from those of other competitive reaction paths, though the (γ,π^+xn)

products are not separable from the (γ,p*x*'n) products. The information obtained from the activation method is integral with respect to the energy and angle of the final products, but forgoes a detailed theoretical analysis of the final states involved. However, the complete picture concerning competitive reaction paths opened by Δ-resonance such as photopion reactions different in *x*, photospallation, photofragmentation and photofission in cases of heavy complex nuclei can be clarified. A series of radiochemical measurements of photonuclear reactions of complex nuclei in the Δ region has been performed and systematized with respect to photon energy and target mass during the last 25 years. The present paper is a concise review of the part of photopion reactions among the various reaction paths opened by the Δ-resonance. Our study of the (γ,π^-xn) reactions emphasizes the yield variations for individual *x* with respect to a wide range of photon energies and target compositions, A_t and $(N/Z)_t$. The (γ,π^+) yields relative to the (γ,π^-) yields over the same range of photon energies and target compositions are another concern in the present work. The results are also discussed in conjunction with a theoretical calculations based on the photon-induced intranuclear cascade analysis code (PICA) by Gabriel and Alsmiller [5].

2. Experimental

All of the data included in this paper were obtained from bremsstrahlung irradiations of targets (^{7}Li–^{209}Bi) in suitable chemical forms using the 1.3 GeV electron synchrotron of the High Energy Accelerator Research Organization (KEK) at Tanashi in the bremsstrahlung end-point energies E_0 range of 250–1200 MeV, and the 300 MeV electron linac of the Laboratory of Nuclear Science, Tohoku University in the E_0 range of 30–270 MeV, both using steps of 50 MeV or less. For the experimental detail and the data analysis, see Ref. [1–4].

3. Results and Discussion

3.1. Mass Yield Distribution

Measured (secondary-corrected) yields as a function of E_0, $Y(E_0)$, in unit of μb per equivalent quanta (μb/eq.q.), show steep rises above E_0 = 140 MeV, the photopion threshold, and attain plateaus around E_0 = 300–500 MeV, which are characteristic of the resonance process. Typical examples of the yield curves $Y(E_0)$ and of the cross sections per photon of energy, *k*, $\sigma(k)$, obtained by unfolding of $Y(E_0)$ were reported for ^{51}V [1] and ^{133}Cs [2] targets. In the following the energy-integrated $Y(E_0)$ values are presented to characterize their target dependent features. The E_0-dependence of the (γ,π^-xn) yields is shown in Fig. 1, where the measured yield values at E_0 = 800, 400 and 250 MeV from ^{51}V, ^{59}Co, ^{75}As, ^{89}Y, ^{109}Ag, ^{115}In, ^{127}I, ^{133}Cs, ^{139}La, ^{175}Lu, ^{197}Au and ^{209}Bi targets are plotted as a function of the number of neutrons emitted (*x*), i.e., isotopic mass yield curves. The solid, broken and dotted curves are drawn through the data points for E_0 = 800, 400 and 250 MeV, respectively, taking the target mass-dependent variations of all the yield values into consideration. The mass yields at E_0 = 400 and 800 MeV are almost the same and higher than those at E_0 = 250 MeV. The difference between the yield patterns for 250 MeV and 400 (and 800) MeV increases with the increasing A_t, and it becomes more prominent at larger *x* in the A_t region from 127 to 209. An important feature of the isotopic mass yield curves is that the reactions of high neutron multiplicities become progressively more possible as A_t increases, and the reaction probabilities for *x* = 2–7 (and even more) at $E_0 \geq$ 400 MeV are nearly comparable for a heavy target such as ^{175}Lu, ^{197}Au or ^{209}Bi, though not at E_0 = 250 MeV. On the other hand, reactions with such high neutron multiplicities are not possible for the lighter targets (A_t < 100). For the region of targets having A_t = 51–115, as shown in the upper half of Fig. 1, the difference between the 250 MeV and the 400 (and 800) MeV yields is more prominent at *x* = 1–3. The neutron multiplicity reflects primarily the excitation energy left after pion emission, while the energy spectrum of neutrons is to be known. Also noteworthy is that the yields for (γ,π^-) reactions are almost the same for all of the studied targets at E_0 = 800, 400 and 250 MeV.

The widths of the mass yield distributions at E_0 = 400 and 250 MeV, defined here as the *x* values of the (γ,π^-xn) reaction for which the yield is equal to that of the (γ,π^-) reaction, 78 μb/eq.q. for E_0 = 400 MeV and 51 μb/eq.q. for E_0 = 250 MeV (see subsection 3.2 below), are read from the fit curves in Fig. 1 and plotted as a function of the neutron-to-proton ratio of the target, $(N/Z)_t$, in Fig. 2. The target dependence of the yields from the (γ,π^-xn) reactions for $x \geq 1$ is not parameterized by target mass A_t, nor by the number of target neutrons N_t, because the (γ, π^-2n) and (γ, π^-3n) reaction yields from ^{51}V are higher by an order of magnitude than those from ^{59}Co, as seen in the upper left corner of Fig. 1. As noted above qualitatively, the range of neutron multiplicity is larger for heavier targets. However, the degree of the increase of the width is not monotonic, but changes largely at $(N/Z)_t$ = 1.3–1.4 (^{109}Ag-^{127}I), and the rate of increase becomes smaller at $(N/Z)_t$ = 1.30–1.35 (^{109}Ag–^{115}In) and at 1.48–1.52 (^{197}Au–^{209}Bi) in the case of E_0 = 400 MeV. The change of the width at E_0 = 250 MeV is small, but the rate of increase also changes at $(N/Z)_t \approx 1.35$. The peak positions also increase with an increasing of $(N/Z)_t$ in a manner similar to the widths (see the discussion on (γ,π^-xn) yields below).

3.2. ($\gamma,\pi^{\pm}$) Yields

Figure 3 shows the measured yields (large symbol) of (γ,π^+) and (γ,π^-) reactions at E_0 = 400 MeV as a function of A_t, together with the literature data (small symbols) [4]. Open squares are for the (γ,π^+) yields from ^{9}Be, ^{27}Al, ^{37}Cl, ^{41}K, ^{51}V, ^{59}Co, ^{60}Ni, ^{65}Cu, ^{75}As, ^{87}Rb, ^{88}Sr, ^{109}Ag, ^{115}In, ^{133}Cs, ^{138}Ba, ^{139}La and ^{181}Ta, and closed circles for the (γ,π^-) yields from ^{7}Li, ^{11}B, ^{12}C, ^{14}N, ^{44}Ca, ^{51}V, ^{65}Cu, ^{75}As, ^{88}Sr, ^{89}Y, ^{127}I, ^{130}Te, ^{133}Cs, ^{139}La, ^{175}Lu, and ^{197}Au, and they are connected by solid lines, respectively. Dotted lines are the corresponding ones calculated by the PICA code. Both the ($\gamma,\pi^{\pm}$) yields are A_t-independent except for light targets, irrespective of E_0. The yields for (γ,π^-) reactions on lighter targets such as ^{7}Li, ^{11}B, ^{12}C, ^{14}N are anomalously small compared with those for the heavier targets. The low values for the ^{7}Be and ^{14}O yields up to E_0 = 1200 MeV were confirmed in the present work, and the low yields are explained as due to small numbers of particle stable states (two in ^{7}Be, ten in ^{11}C, one in ^{12}N and ^{14}O) [6]. Also, it is well known that the anomalously slow transition rates in the A = 14 isobars are observed in $^{14}\mathrm{C} \rightarrow {}^{14}\mathrm{N} + e^- + \bar{\nu}_e$ and $^{14}\mathrm{O} \rightarrow {}^{14}\mathrm{N} + e^+ + \nu_e$ as well as in radiative pion and muon captures [7]. On the other hand, many bound states leading to (γ,π^-) reactions exist for the heavy nuclei. This manifests the A_t-independence in the heavy target region; the weighted means of the yield values of (γ,π^-) reactions on targets having $A_t \geq 44$ are 91±6, 78±6 and 51±5 μb/eq.q. for E_0 = 800, 400 and 250 MeV, respectively (horizontal solid lines in Fig. 3). The PICA calculations for the corresponding reactions on these heavy targets at E_0 = 400 MeV are smaller than the measured values by 35 % on average, though the calculations also indicate A_t-independence. The (γ,π^+) reaction yields are also A_t-independent for $A_t \geq 27$, and their weighted means are 18±2, 14±2, 7.3±1.1μb/eq.q. for E_0 = 800, 400 and 250 MeV, respectively. The yield values reported for ^{9}Be(γ,π^+)^{9}Li in the energy range of E_0 = 100-800 MeV by Nilsson *et al.* [8] are definitely smaller than the trend, probably because there are only two bound states in ^{9}Li. Although both the (γ,π^+) and (γ,π^-) reactions on the light nuclei have been of interest from a theoretical point of view [9], they are not included in our discussions with those of the heavier complex nuclei which allow for statistical treatments. The PICA calculation for (γ,π^+) reactions in the heavy target region also reproduces the A_t-independence, but the average values obtained from the calculations are two times those of the measurements. Thus, the measured yields in the A_t-independent region at E_0 = 400 MeV give a yield ratio of $Y(\gamma,\pi^-)/Y(\gamma,\pi^+)$ = 5.6±1.0, while the corresponding PICA value at E_0 = 400 MeV is 1.8±0.3.

The high observed yield ratios compared with the calculated ones may imply new nuclear structure effects that are not taken into consideration in the theoretical foundation of the PICA code. The nuclear model used in the theoretical calculations is exactly the same as the one used in the Bertini calculations [10]. The continuous charge density distribution inside the nucleus, $\rho(r) = \rho_0/\{1+\exp(r-c)/z_1\}$, c and z_1 being the relevant parameters, obtained by electron scattering data [11] was approximated by dividing the nucleus into three concentric spheres: a central sphere and two surrounding spherical annuli having the uniform densities of 0.9, 0.2, and 0.01 of $\rho(0)$ at the center of the nucleus. The neutron to proton density ratios were assumed to be equal to the ratio of neutrons to protons for the entire nucleus. Cross sections for the photoabsorption by a nucleon in the (3,3) resonance region were taken from those for elementary processes for free nucleon-photon interactions, by assuming $\sigma(\gamma p \rightarrow n\pi^+) = (\gamma n \rightarrow p\pi^-)$ from charge-symmetry considerations. And the intranuclear cascade calculation of Bertini [10] was then used to account for the secondary effect of nucleon- and pion-interactions with the remaining nucleus following the initial photon interaction. Pion absorption is assumed to occur via a two-nucleon mechanism with a cross section for the absorption of a charged pion by a nucleon with isobaric spin projection of the opposite sign (i.e., a pair of nucleons must contain at least one proton to absorb a negative pion and at least one neutron to absorb a positive pion).

The higher yields of the (γ,π^-) reactions and the lower ones of the (γ,π^+) reactions relative to those expected from the PICA calculation could possibly be understood if the neutron density in nuclear surface region is higher than the inner density of the nucleus. An initial production of negative pions by way of $\gamma + n \rightarrow \Delta^0 \rightarrow p + \pi^-$ would be more probable than those of positive pions by way of $\gamma + p \rightarrow \Delta^+ \rightarrow n + \pi^+$, and the secondary absorption of negative pions by way of $\pi^- + pp$ or $\pi^- + pn$ would be less than those for positive pions by way of $\pi^+ + np$ or $\pi^+ + nn$ in the neutron-rich surface region.

These processes which lead to (γ,π^-) and (γ,π^+) reactions are, therefore, considered here to occur in the surface region of the nucleus, but experimental observations seem to show that the cross sections are not proportional to $A_t^{2/3}$ but A_t-independent. This A_t-independence may be explained as due to a compensation for the increase in pion production with increasing nuclear size (surface) by the competitive increase of neutron emissivity associated with pion emission (see subsection 3.3). The available final transitions are, therefore, limited to a certain number of levels below the particle separation energy which is set equal to 7 MeV in PICA. While the number of the bound states and the strength of transitions to these states are unknown, they must be statistically significant, as the A_t-independence from the PICA calculation also suggests. There has been no

evidence for the density difference between protons and neutrons in the stable nucleus, but neutron skin and neutron halo structures have been discovered in very neutron-rich light nuclei near the drip line [12, 13]. Further study of structural changes in nuclei closer to the stability line is required; the present work suggests photonuclear processes may cause such effects.

3.3. $(\gamma,\pi^- x\mathrm{n})$ Yields

In order to reveal the target-dependent changes of the $(\gamma,\pi^- x\mathrm{n})$ reaction yields for each x of $x \geq 0$, the yield values at E_0 = 400 MeV (closed squares) are plotted in Fig. 4 as a function of the neutron-to-proton ratio of the entire target nucleus, $(N/Z)_t$. Solid lines representing x = 0–9 are drawn through the observed points with the aid of the smoothed mass yield curves in Fig. 1. Also plotted in Fig. 4 are the yield values calculated for E_0 = 400 MeV (open circles) by the PICA code [4].

The yield values of the $(\gamma,\pi^- x\mathrm{n})$ reactions at a given E_0 change systematically with respect to the neutron multiplicity x and $(N/Z)_t$. Both the observed and the calculated values for the individual reactions begin at a certain $(N/Z)_t$, increase rapidly with an increase of $(N/Z)_t$, and reach a plateau. The PICA calculations approximate the observed profiles as a whole. Notably, the positive slope regions of the $Y(E_0)$ vs. $(N/Z)_t$ curves are well reproduced, with some exceptions at $(N/Z)_t$ = 1.18 (^{59}Co), 1.32 (^{109}Ag), 1.35 (^{115}In), whereas the plateau values are largely discrepant. The PICA results underestimate by 35% the (γ,π^-) yields as noted above, but increasingly overestimate by factors of 1.5–2.0 the $(\gamma,\pi^- x\mathrm{n})$ reaction yields for $x \geq 3$. The deviation increases with the increasing x. The calculations for light targets such as ^{7}Li, ^{11}B, ^{12}C, ^{14}N and ^{27}Al, for which observed values for either the (γ,π^-) or (γ,π^+) reactions are available, show small yields for reactions with x = 1–2, but show large deviations from the smooth trends of the yields for the heavier targets. Also it was found that the start values of $(N/Z)_t$, the slopes of the rising part, and the plateau values indicate smooth variations with respect to x, but all change their variations at $x \geq 5$. Also the sums of the yields of the reactions of x = 0 to 1, 2, ···, 9 and the maximum possible x (max), $\sum^{x}_{i=0} Y_i(N/Z)_t$, increase sigmoidally with an increase of $(N/Z)_t$, showing that the $\sum^{max}_{i=0} Y_i(N/Z)_t$ curve consists of two sigmoides; one from $(N/Z)_t$ = 1.01 to 1.35 and the other from 1.35 to 1.55. The second sigmoid is steep, reflecting the rapid increase in the $(\gamma,\pi^- x\mathrm{n})$ yields for $x \geq 5$ for the targets with $(N/Z)_t \geq 1.35$. All of these changes in the yield profiles for targets heavier than A_t = 100 might be associated with pronounced nuclear medium effects giving rise to more excessive excitation as compared with medium-heavy targets of $A_t \leq 100$. A more advanced theoretical model concordant with the present findings needs to be developed in order to better quantify the results.

Acknowledgement

The authors would like to express their gratitude to Drs. H. Okuno and K. Masumoto, and the ES crew members of the High Energy Accelerator Research Organization at Tanashi, for their invaluable cooperations in the course of experiments. This work was supported in part by the Grant-in-Aid for Scientific Research (07304077) of the Ministry of Education, Science and Culture of Japan.

References

[1] Sakamoto, K., Yoshida, M., Kubota, Y., Fukasawa, T., Kunugise, A., Hamajima, Y., Shibata, S., and Fujiwara, I.: Nucl. Phys. **A501**, 693 (1989).
[2] Sakamoto, K., Hamajima, Y., Soto, M., Kubota, Y., Yoshida, M., Kunugise, A., Masatani, M., Shibata, S., Imamura, M., Furukawa, M., and Fujiwara, I.: Phys. Rev. C**42**, 1545 (1990).
[3] Oura, Y., Yazawa, A., Yoshida, M., Sarkar, S. R., Sakamoto, K., Shibata, S., Fujiwara, I., and Furukawa, M.: Radiochim. Acta **68**, 27 (1995).
[4] Sakamoto, K., Sarkar, S. R., Oura, Y., Haba, H., Matsumura, H., Miyamoto, Y., Shibata, S., Furukawa, M., and Fujiwara, I.: Phys. Rev. C **59**, 1497 (1999).
[5] Gabriel, T. A. and Alsmiller, Jr., R. G.: Phys. Rev. **182**, 1035 (1969).
[6] Oura, Y., Kawaguchi, K., Sarkar, S. R., Haba, H., Miyamoto, Y., Sakamoto, K., Shibata, S., Fujiwara, I., and Furukawa, M.: Res. Rept. Lab. Nucl. Sci. Tophoku Univ. **27**, 133 (1994).
[7] Blomqvist, I., Nydahl, G., and Forkman, B.: Nucl. Phys. **A162**, 193 (1971).
[8] Nilsson, M., Schroder, B., Bulow, B., Grintals, J., Jonsson, G. G., Lindner, B., Srinivasa Rao, K., and Susila, S.: Z. Physik **A294**, 253 (1980).
[9] Nagl, A., Devanathan, V., and Uberall, H.: *Nuclear Pion Photoproduction* (Springer-Verlag, Berlin 1991).
[10] Bertini, H. W.: Phys. Rev. **131**, 1801 (1963).
[11] Hofstadter, R.: Rev. Mod. Phys. **28**, 214 (1956).
[12] Hansen, P. G., Jensen, A. S., and Jonson, B.: Ann. Rev. Nucl. Part. Sci., **45**, 591 (1995).
[13] Tanihata, I.: J. Phys. G: Nucl. Part. Phys. **22**, 157 (1996).

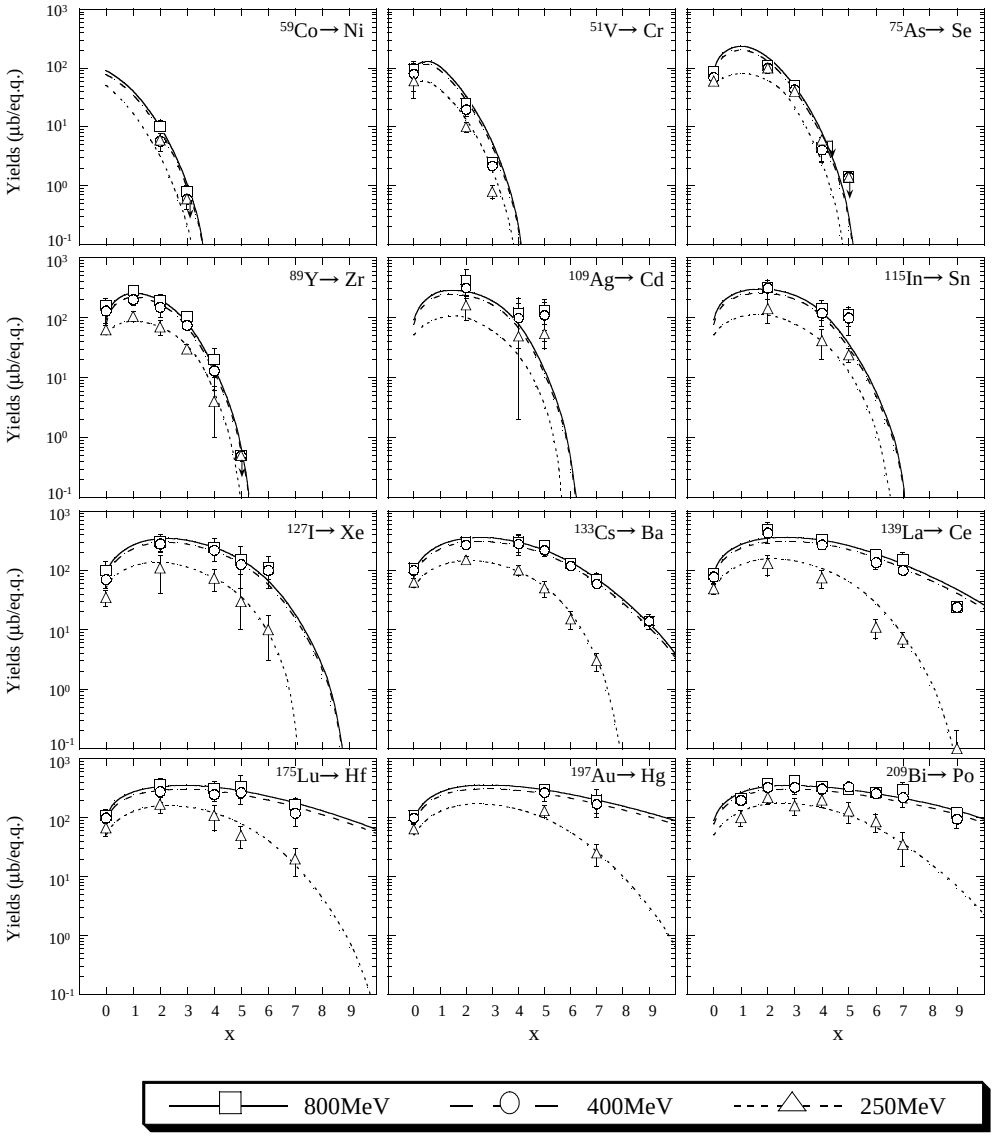

Fig. l. Variations for (γ,π^-xn) reaction yields in unit of μb/eq.q. as a function of number of emitted neutrons, x, isotopic mass yield curves, at E_0=800, 400, and 250 MeV.

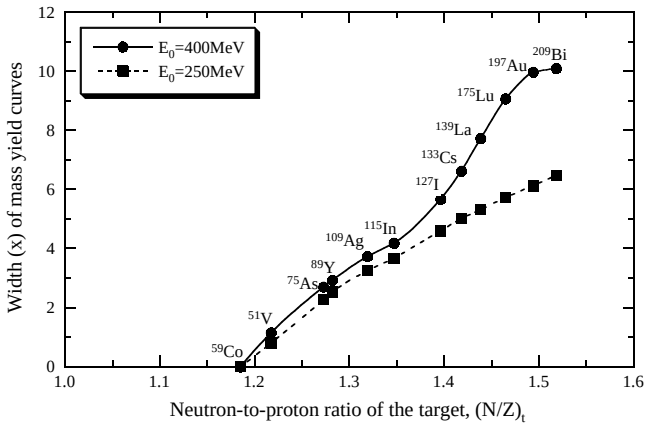

Fig. 2. Widths of the isotopic mass yield curves as a function of $(N/Z)_t$ at E_0=400 and 250 MeV.

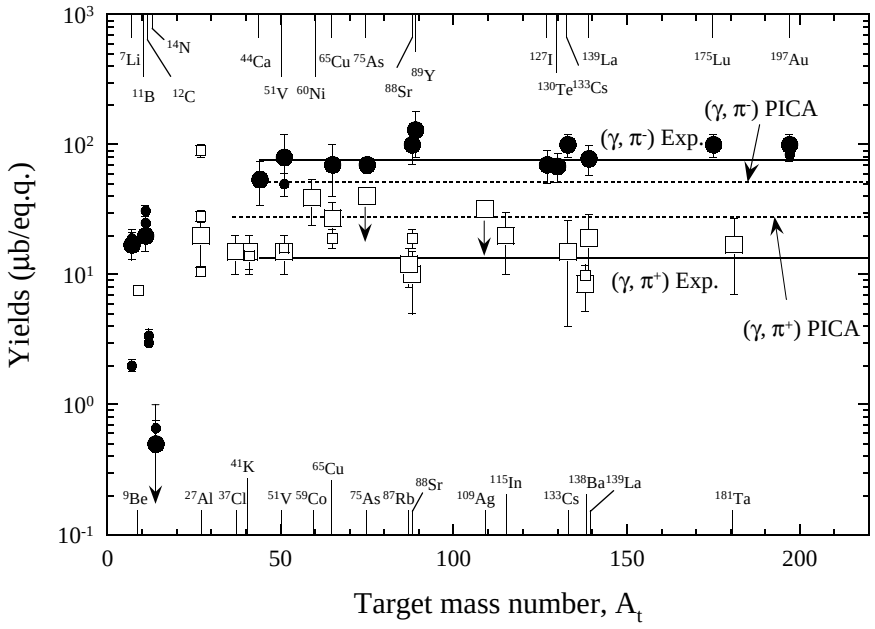

Fig. 3. Variations of the measured and calculated yields for the (γ,π^+) and (γ,π^-) reactions as a function of A_t at E_0 = 400 MeV. See the text for explanation.

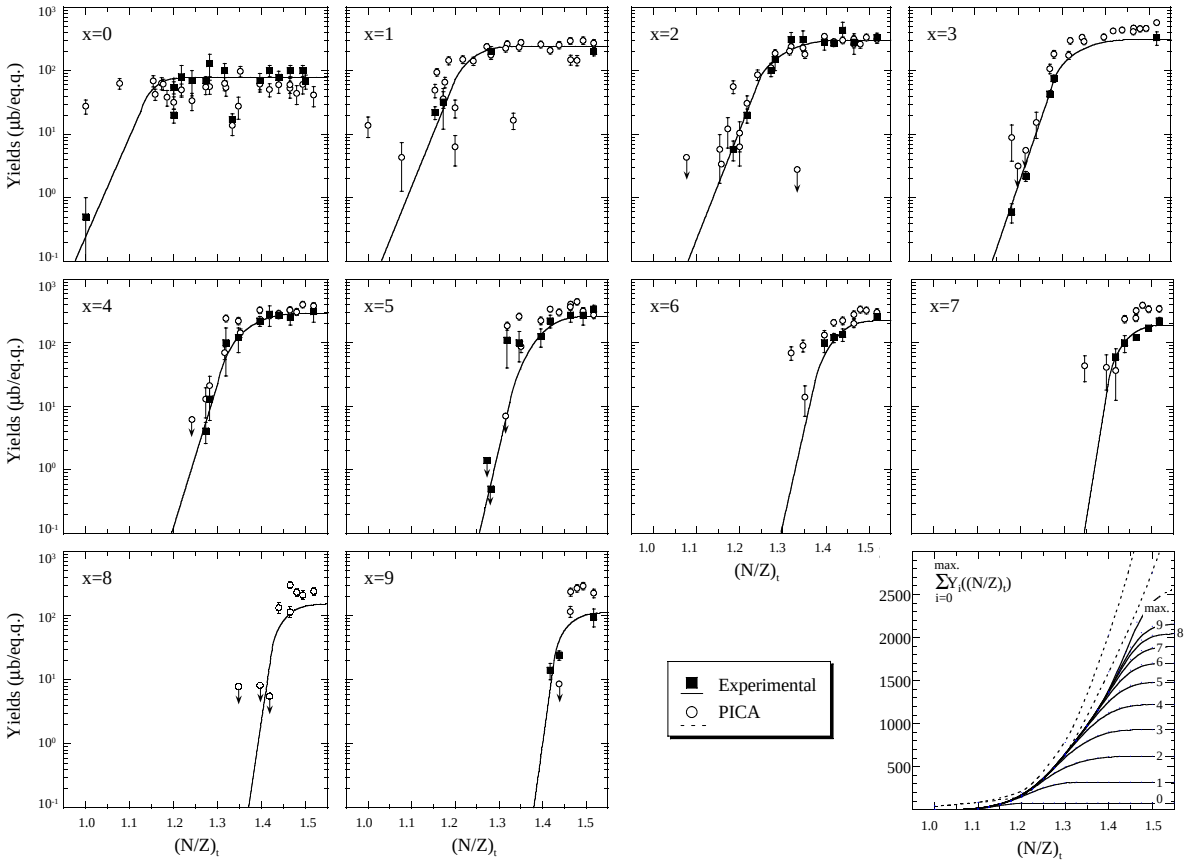

Fig. 4. Variations of the measured and calculated yields for the (γ,π^-xn) reactions as a function of $(N/Z)_t$ at E_0 = 400 MeV. See the text for explanation.